Supporting Information

Synergistic Material Modifications Induced Optimization of Interfacial Charge Transfer and Surface Hydrogen Adsorption

Mingyan Du,[a,†] Lingling Cui,[a,†] Panpan Wang,[b,†] Chunyao Niu,[b,] Young Soo Kang[c] and Xiao Li Zhang[a,*]*

[a]School of Materials Science and Engineering, Zhengzhou University, 450001 P.R. China.

[b]*School of Physics and Microelectronics, Zhengzhou University, 450001 P.R. China.*

[c]*Environmental and Climate Technology, Korea Institute of Energy Technology (KENTECH), 200 Hyeoksin-ro, Naju City, Jeollanamdo 58330, Korea.*

*Corresponding authors. E-mail: xiaolizhang.z@gmail.com.

Experimental Details

Chemicals

All chemicals used in the material syntheses were reagent grade including sodium hydroxide, ethanol, nickel nitrate (98%), hydrochloric acid (37%), glucose (98%), ammonium fluoride and methanol from Sinopharm Chemical Reagent Co., Ltd (Shanghai, China) and Degussa P25 TiO_2 nanoparticles from Evonik. Milli-Q water (18.2 mΩ/cm) were used throughout the experimental work.

Materials synthesis

To form an Ni-substituted TiO_2 the following approach was used.[1] Preparation of Ni doped TiO_2 (NT): P25 TiO_2 nanoparticles (0.5 g) was dispersed in a 5 M sodium hydroxide aqueous solution (30 mL) before being transferred into a Teflon-lined stainless-steel autoclave (50 mL in capacity) for hydrothermal reaction at 140°C for 10 h. The products were rinsed several times with water to remove residual sodium hydroxide and collected by centrifugation before being redispersed in 500 mL of 0.1 M hydrochloric acid solution. The precipitates were centrifugated and redispersed into 30 mL of aqueous solution containing nickel nitrate with various concentration (following a Ni/TiO_2 ratio of 0, 0.5, 1.0, 2.0 and 3.0 wt%). The products were then collected by centrifugation and rinsed with water and ethanol several times before being dried under vacuum at room temperature, obtaining nickel titanates with varying nickel doping concentrations. With temperature ramping rate of 2°C/min to 450 °C, the samples were calcined in a muffle furnace for 2 h in air and labelled as NT0 (pure TiO_2), NT0.5, NT1, NT2, and NT3, corresponding to the increasing nickel doping concentrations (0, 0.5, 1.0, 2.0 and 3.0 wt%).

Carbon coating of NTx were prepared as follow. 0.2 g NT2 was dispersed into 30 mL aqueous solution with 0.2 ml glucose aqueous solution (C:Ni=1:1) by sonication before hydrothermal reaction at 150 °C for 15 h in a 50 mL Teflon-lined stainless-steel autoclave. The products were rinsed by water and ethanol several times before being collected by centrifugation and dried at 60 °C for 10 h and denoted as CNTx - CNT0, CNT0.5, CNT1, CNT2 and CNT3, respectively, corresponding to the Ni-content. Carbon content was also investigated on the NT2 sample with Ni:C ratios of 2:1, 2:2 and 2:4.

Fluorinated carbon capping of NTs were prepared using glucose and ammonia fluoride aqueous solution instead following the same process as carbon capping of the NTx with F: C: Ni of 1:2:2. The corresponding products were labelled as FNT0 (fluorinated carbon encapsulation of pure TiO_2), FNT0.5, FNT1, FNT2, and FNT3, respectively.

Characterization

A transmission electron microscope (TEM, JEM-2100F, JEOL) were used to investigate the morphology and conduct elemental mapping of the samples. X-ray diffraction (XRD) patterns of the obtained samples were obtained on an X-ray diffractometer (UItima IV) using Cu Kα irradiation under a 40 kV working voltage and were used to determine the phase structures. Raman spectra were acquired on a HORIBA Lab-RAM HR-Evolution Raman spectrometer with laser excitation at 532 nm. The UV/Vis diffuse reflectance spectra (UV/Vis DRS) were obtained with a UV/Vis/NIR spectrophotometer (UH4150, Hitachi, Japan) in the wavelength range 300-800 nm. The photoluminescence spectra were recorded on a fluorospectrometer (F-280-Laser-NIR, Gangdong Science and Technology Development Co., LTD. Tianjin) with an excitation wavelength of 460 nm. X-ray photoemission spectra (XPS) were collected using a Thermo Escalab 250xi analyzer. Binding energies of Ti 2p, O 1s, C 1s and F 1s were recorded using Al Kα (1486.6 eV) as the excitation source and a pass energy of 23.5 eV. The position of the XPS peaks of the corresponding element is referenced to the C1s peak.

Photocatalytic hydrogen generation

The photocatalytic hydrogen evolution experiments were carried out at room temperature (20 ± 1 °C) controlled by a cooling system and in a vacuum sealing reaction system. 10 mg of the powdered photocatalyst was dispersed in a 50 mL of 10% methanol aqueous solution by ultrasonication in a Pyrex flask (350 mL) equipped with a water jacket to exclude the temperature influence from illumination. Top illumination mode was used with a 300 W Xe lamp (Perfect Light, PLS-SXE300D) through the flat window of the reactor. Gas evolution was determined by an online gas chromatograph (GC-7860, Ar carrier gas).

Electrochemical measurement

The electrochemical catalytic performance throughout the measurement process was conducted in 0.5 M Na_2SO_4 solution using a (CHI 760E Electrochemical Workstation) with a three-electrode system. A platinum plate (1 × 1 cm^{-1}), a saturated Hg/Hg_2Cl_2 electrode and a fluorine doped tin oxide (FTO) coated glass plate (1 × 1 cm^{-1}) were used as the counter, reference and working electrode, respectively.

The working electrode was prepared for testing samples, PVDF and NMP. In detail, a mixture of 300 mg sample, 2.7 g PVDF and 1 mL NMP were moderately stirring overnight before being coated on FTO, then calcination under 400 °C for 1h.

Computational simulation details

All calculations were based on the first principles of density functional theory (DFT) and performed by the Vienna Ab-initio Simulation Package (VASP).[2, 3] The exchange correlation energy was calculated by Perdew-Burke-Ernzerhof (PBE) of generalized gradient approximation (GGA).[4] The DFT-D3 method was used to describe the vdW interactions,[5, 6] and the DFT+U method was used to more accurately describe the Coulomb interaction of the system, setting the effective U value on the Ti 3d orbit to 4.2 eV.[7, 8] The vacuum space was set to 15 Å to avoid the interaction between two periodic units. The plane wave energy cut-off was set to 450 eV and k-point was set to $2 \times 4 \times 1$. A total energy convergence of 10^{-4} eV was used for the calculation of the electron self-consistent field. The TiO_2 (101) surface was modeled with a (2×2) three-Ti-layer slab (24 Ti and 48 O atoms), the heterogeneous junction structure was modeled using a (2×2) supercell of TiO_2 (101) surface and a (5×3) graphene supercell, and the distance between the graphene layer and the TiO_2 (101) surface is 2.8 Å. One Ni atom is doped in the TiO_2 surface model, corresponding a Ni doping concentration of ~4%, which is comparable to the experiments results (0.5~3wt%). In all structures, the bottom eight atoms (four oxygen and four titanium) were fixed.

The solvation effect is not taken into account in the calculations as our goal is to investigate the effects of Ni-doping, carbon shield, and further fluorine-doping of the thin carbon shield on the tendency of TiO_2 photocatalytic HER activity. Despite the solvation effect may have some influence on the adsorption energy of hydrogen, but the trend of TiO_2 photocatalytic activity will be maintained.

The adsorption energy and Gibbs free energy change of hydrogen adsorption was defined as:

$$\Delta E_{H*} = E_{H*cat} - E_{cat} - \frac{1}{2}E_{H_2}$$

$$\Delta G_{H*} = \Delta E_{H*} + 0.24$$

where E_{H*cat} and E_{cat} is the energies of the catalyst with and without H adsorption, respectively. E_{H_2} is the energy of the molecular hydrogen in the gas phase, and 0.24 is the free energy correction, which was proposed by Norskov et al.

The adsorption energy of hydroxyl was calculated by the following formula:

$$\Delta E_{OH*} = E_{OH*cat} - E_{cat} - E_{OH}$$

where E_{OH*cat} and E_{cat} is the energies of the catalyst with and without OH*, respectively. E_{OH} is the energy of hydroxyl.

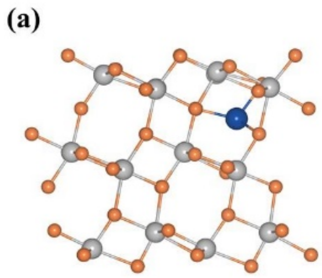

Figure S1. The most stable position for Ni atoms doped in TiO_2: (a) $Ni_a@TiO_2$, (b) $Ni_b@TiO_2$

Table S1. The adsorption energy of hydroxyl and hydrogen on TiO_2 and Nia/TiO_2.

	TiO_2		Ni_a/TiO_2	
	O site	Ti site	O site	Ti site
E_{H*} /eV	0.37	-	0.29	-
E_{OH*} /eV	0.26	-1.12	0.15	-3.47

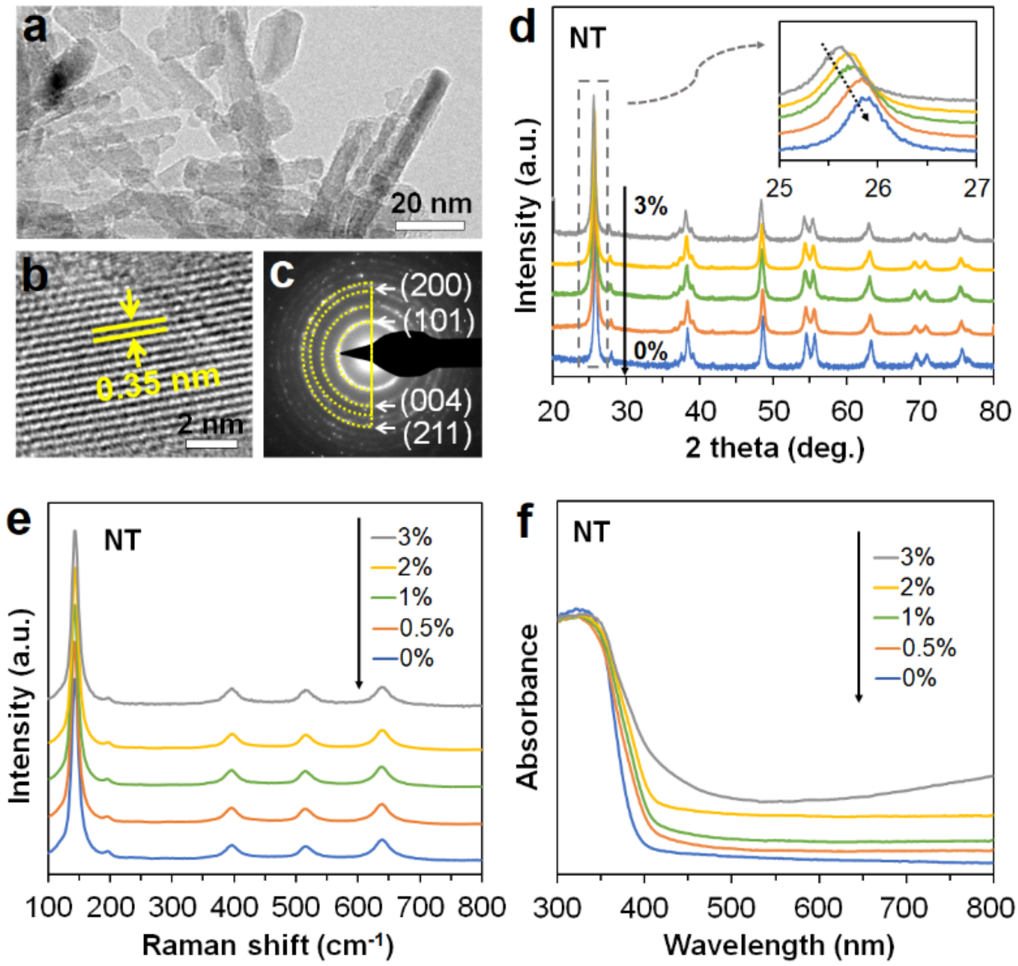

Figure S2. (a-c) TEM, HR-TEM and SAED images of 2% Ni-doped TiO_2, NT2; (d-f) XRD, Raman and UV-visible diffuse reflectance spectra of NTs for a varying Ni-doping level.

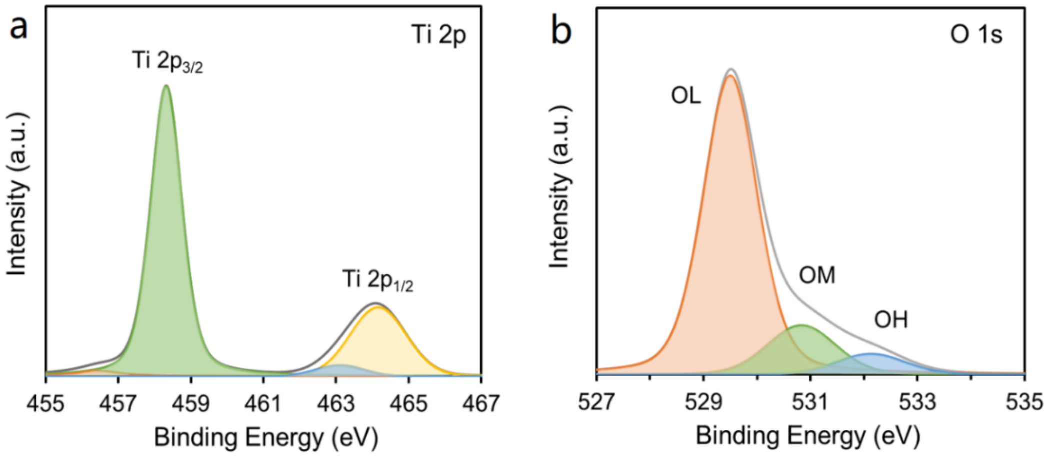

Figure S3. XPS analyses of (a) Ti 2p, (b) O 1s for TiO_2 (NT0).

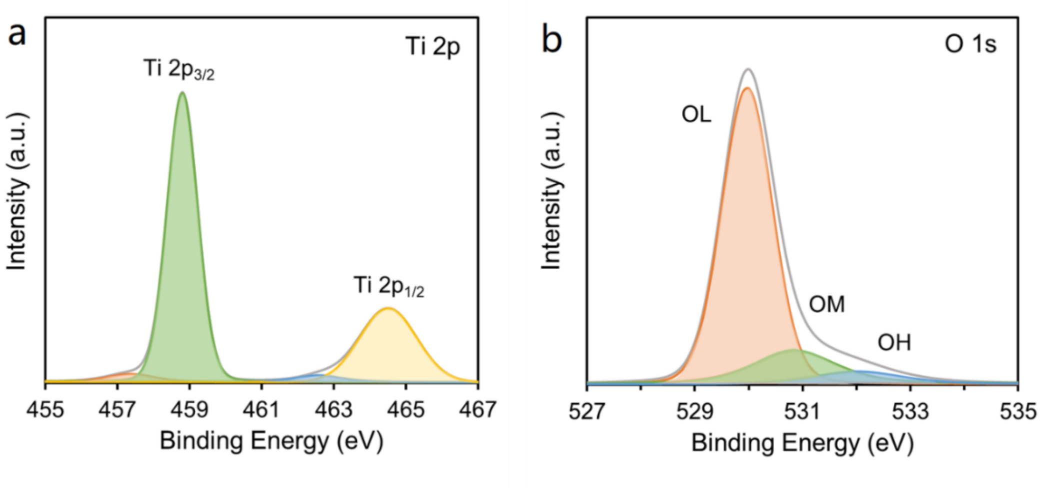

Figure S4. XPS analyses of (a) Ti 2p, (b) O 1s for NT2.

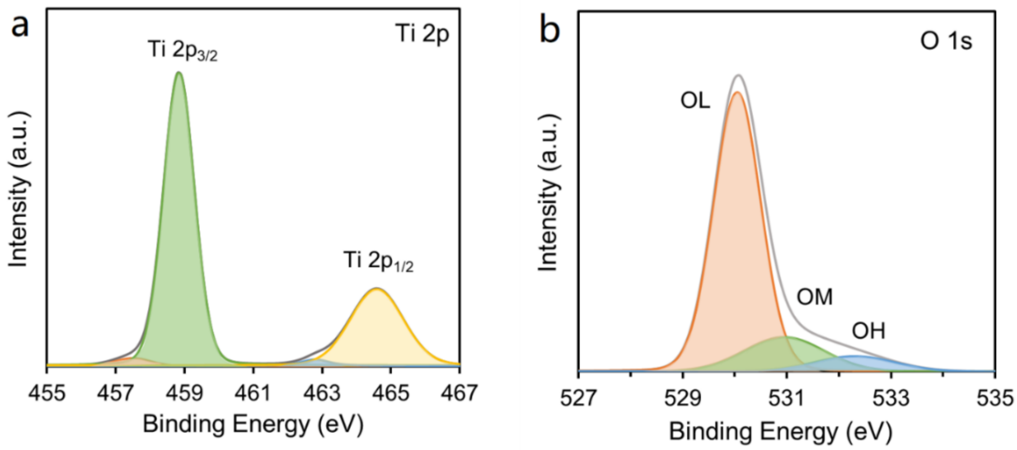

Figure S5. XPS analyses of (a) Ti 2p, (b) O 1s for CNT2.

Table S2. Detailed analysis of Ti^{3+}, oxygen vacancy (Ov), surface hydroxyl groups (OH) contents (%) in various catalysts from XPS spectra.

Sample	Ti^{3+}	O_V	OH
TiO_2	5.7	14.8	6.1
NT2	6.0	16.8	6.4
CNT2	3.5	15.6	6.9
FNT2	2.8	12.8	7.0

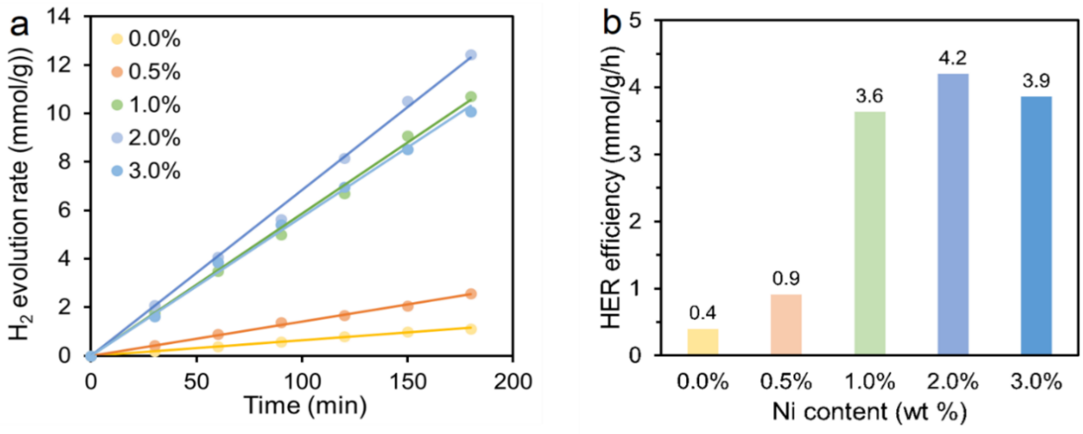

Figure S6. (a) H_2 evolution rate, and (b) HER efficiency of NTx with varying Ni-doping level.

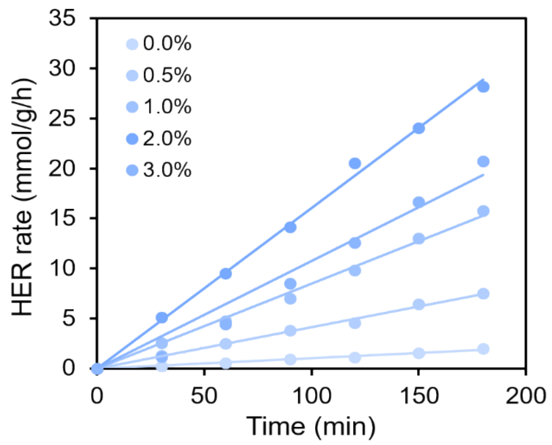

Figure S7. (a) H_2 evolution rate of CNTx with varying Ni-doping level.

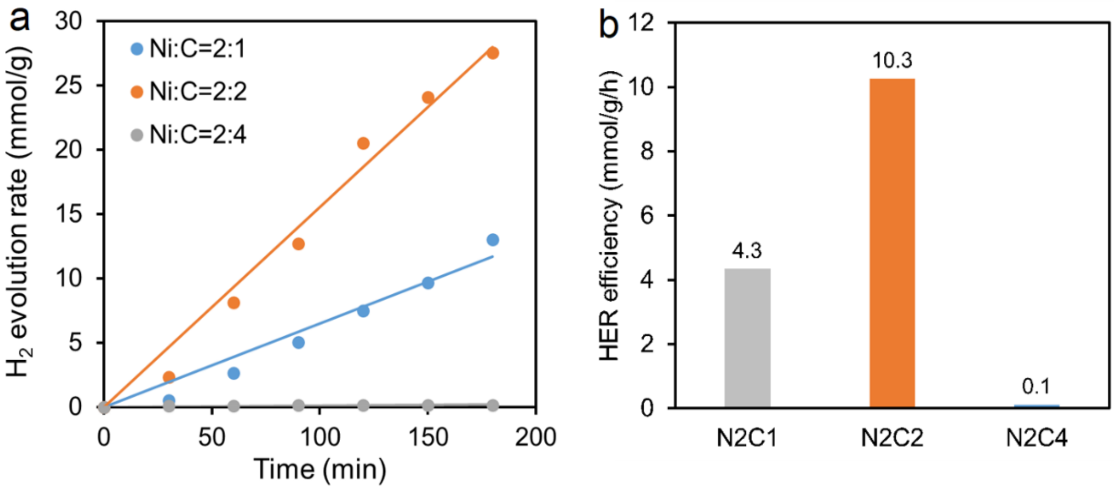

Figure S8. (a) H_2 evolution rate, and (b) HER efficiency of the CNT2 as a function of the carbon content.

Table S3. Comparison of photocatalytic activity in hydrogen production of recent metal-doped TiO_2 photocatalysts composites.

Photocatalyst	Concentration (mg/ml)	Reactant solution	HER rate (mmol/g/h)	Incident light	Ref.
FNT2	0.2	10 % methanol	13.00	300 W xenon lamp	This work
Ni/TiO_2	0.2	50 % methanol	3.39	450 W Hg lamp	[9]
$Ni/TiO_2/C$	0.8	20% methanol	3.56	300 W Xenon lamp	[10]
Mg/TiO_2	0.2	100 % water	0.85	AM 1.5 G solar simulator	[11]
Ga-TiO_2 nanoparticles	1	20 % methanol	5.77	150 W xenon arc lamp	[12]
Co/TiO_2	2	5% glycerol	11.02	400 W Hg vapor lamp	[13]
single atom Cu-TiO_2	0.065	25 % methanol	16.60	Xenon lamp (100 mW/cm^2）	[14]
Cu-TiO_2/C	0.25	10 % methanol	14.40	365 nm LED (80 mW/cm^2)	[15]
TiO_2/Pt/rGO	1	20 % methanol	0.48	Philips PL-S lamp (315 - 400 nm)	[16]
Pt/TiO_2	5	20 % methanol	11.20	AM 1.5 G solar simulator	[17]
Pt/TiO_2	0.5	25 % methanol	19.22	400 W Xenon lamp	[18]

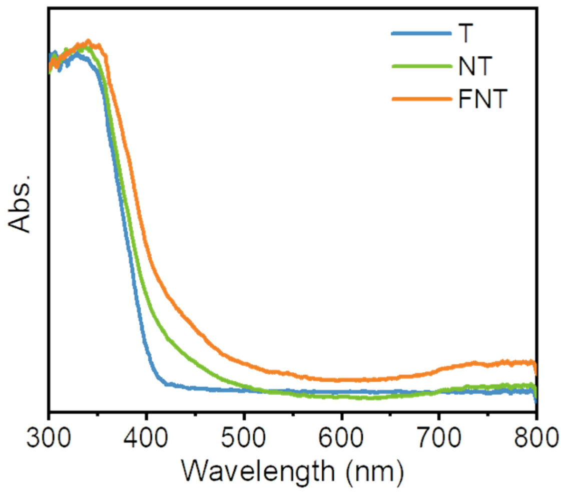

Figure S9. UV-vis absorption spectra of pure TiO_2, NT2 and FNT2.

REFERENCES

1 B. Guan, J. Yu, S. Guo, S. Yu and S. Han, *Nanoscale Adv.*, 2020, **2**, 1352-1357.

2 G. Kresse and J. Hafner, *Phys. Rev. B*, 1993, **47**, 558-561.

3 G. Kresse and J. Furthmüller, *Phys. Rev. B*, 1996, **54**, 11169-11186.

4 J. P. Perdew, K. Burke and M. Ernzerhof, *Phys. Rev. Lett.*, 1996, **77**, 3865-3868.

5 S. Grimme, S. Ehrlich and L. Goerigk, *J. Comput. Chem.*, 2011, **32**, 1456-1465.

6 S. Grimme, J. Antony, S. Ehrlich and H. Krieg, *J. Chem. Phys.*, 2010, **132**, 154104.

7 L. Yan and H. Chen, *J. Chem. Theory Comput.*, 2014, **10**, 4995-5001.

8 B. J. Morgan and G. W. Watson, *Surf. Sci.*, 2007, **601**, 5034-5041.

9 A. T. Montoya and E. G. Gillan, *ACS Omega*, 2018, **3**, 2947-2955.

10 P. C. Rath, M. Mishra, D. Saikia, J. K. Chang, T. P. Perng and H. M. Kao, *Int. J. hydrog. Energy*, 2019, **44**, 19255-19266.

11 L. Gao, Y. Li, J. Ren, S. Wang, R. Wang, G. Fu and Y. Hu, *Appl. Catal. B*, 2017, **202**, 127-133.

12 S. Luo, T. D. Nguyen-Phan, D. Vovchok, I. Waluyo, R. M. Palomino, A. D. Gamalski, L. Barrio, W. Xu, D. E. Polyansky, J. A. Rodriguez and S. D. Senanayake, *Phy. Chem. Chem. Phys.*, 2018, **20**, 2104-2112.

13 G. Sadanandam, K. Lalitha, V. D. Kumari, M. V. Shankar and M. Subrahmanyam, *Int. J. hydrog. Energy*, 2013, **38**, 9655-9664.

14 B. H. Lee, S. Park, M. Kim, A. K. Sinha, S. C. Lee, E. Jung, W. J. Chang, K. S. Lee, J. H. Kim, S. P. Cho, H. Kim, K. T. Nam and T. Hyeon, *Nat. Mater.*, 2019, **18**, 620-626.

15 L. J. Sun, H. W. Su, D. F. Xu, L. L. Wang, H. Tang and Q. Q. Liu, *Rare Met.*, 2022, **41**, 2063-2073.

16 M. J. Rivero, O. Iglesias, P. Ribao and I. Ortiz, *Int. J. hydrog. Energy*, 2019, **44**, 101-109.

17 B. Banerjee, V. Amoli, A. Maurya, A. K. Sinha and A. Bhaumik, *Nanoscale*, 2015, **7**, 10504-10512.

18 T. L. Soundarya, R. Harini, K. Manjunath, Udayabhanu, B. Nirmala and G. Nagaraju, *Int. J. hydrog. Energy*, 2023, **04**, 289